



Evolution of recrystallization in cold rolled and annealed copper: A texture analysis study

Ghania Benchabane^{1✉}, Hiba Azzeddine², Djamel Bradai³, Zakaria Boumerzoug⁴

1 *Laboratoire de Génie Energétique et Matériaux, LGEM, Université de Biskra, B.P. 145, R.P. 07000, Biskra, Algeria*

2 *Laboratoire Matériaux et Energies renouvelables, Faculté des Sciences, Université Mohamed Boudiaf, M'sila, 28000, Algeria*

3 *Laboratory of Materials Physics, Faculty of Physics, University of Sciences and Technology - Houari Boumediene (U.S.T.H.B.), P.O. Box 32, El- Alia, Bab-Ezzouar, DZ-16111, Algiers, Algeria*

4 *LMSM, Department of Mechanical Engineering, University of Biskra, Biskra, Algeria*

Received January 17, 2024

Revised October 24, 2024

Accepted December 12, 2024

Published online: December 21, 2024

Keywords

Cold rolled copper

Recrystallization

X-ray diffraction

Texture analysis

Harmonic method

ADC method

Abstract: This paper presents a texture analysis study of a cold rolled copper and annealed copper at 450°C for 1 min, 30 min and 100 h. Incomplete poles figures of the studied samples were collected via X-ray diffraction. The experimental data were analyzed after corrections using two methods namely Harmonic and Arbitrarily Defined Cells (ADC). The texture characteristics investigated through orientation distribution function enabled to determine the volume fraction of the prominent texture components. A comparison between results obtained by the two methods shows that the recalculated pole figures and the volume fraction of texture components obtained by the Harmonic and ADC are close. The texture evolution of the cold rolled copper during annealing show that the sharpness of the deformation texture decreased during annealing leading to a dispersed texture in fully recrystallized state (30 min of annealing). The texture after the process of grain growth (100 h annealing) was isotropic and less dispersed compared to the fully recrystallized state.

© 2024 The authors. Published by Alwaha Scientific Publishing Services, ASPs. This is an open access article under the CC BY license.

1 Introduction

Many technologically important materials may undergo mechanical and thermal processes that form a preferred orientation of grains (or crystallographic texture) within the material. This latter has a significant effect on the physical and the mechanical properties of the manufactured material (Wenk and Van Houtte 2004).

Texture analysis using diffraction methods has greatly advanced in the decades because of instrumental and computational developments, and it is now considered as a routine tool for the analysis of grain orientations in a wide variety of materials, including rocks, industrial

products, and archaeological items. This is done using measured pole figures and calculated orientation distribution functions (ODF). These latter are statistically more significant and less prone to biases in the data analysis (Kocks et al. 2000).

Quantitative texture analysis is concerned with detailed analysis of ODF mainly by calculating weight fractions of texture components or texture fibres. These components in turn allow to deduce whether an observed evolution of the microstructure during a thermo-mechanical processing is due to deformation, recrystallization etc. as each of these processes develops typical texture components (Rafailov et al. 2020).

✉ Corresponding author. E-mail address: g.benchabane@univ-biskra.dz.

Several methods have been developed in order to assess the ODF in a polycrystalline sample from pole figures collected by X-ray or neutron diffraction techniques. Two methods are now widely used and are the well-known harmonic method (Bunge 1965; Roe 1965; Roe 1966; Bunge 1982) that is implemented in popLA (Kallend et al. 1991), a texture analysis software package distributed by the Los Alamos Laboratory, and ADC (Arbitrarily Defined Cells) method which is implemented in the LaboTex software (Pawlik et al. 1991).

Many papers dealt with the comparison of the harmonic and vector methods (Esling et al. 1987; Wenk et al. 1987; Matthies et al. 1988; Bacroix et al. 1994; Baudin et al. 1995; Caleyó et al. 2001). For example, Baudin et al. (1995) analyzed the texture of Fe 3% Si sheets of HiB grade at the primary recrystallization state. Globally, the results showed that the volume fraction of texture components, estimated using the harmonic and vector methods, were surprisingly quite close.

In this study, results of texture analysis of cold rolled and annealed copper at 450°C were obtained using Harmonic and ADC methods. The texture was analyzed qualitatively via recalculated pole figure and quantitatively via ODF and volume fraction of texture components determination. This work is the complement of the last studies of the same material (Benchabane et al. 2008; Benchabane et al. 2011) in which microstructural characterization and recrystallization kinetics were determined under dynamic and static annealing at temperatures ranging between 250 and 450°C.

2 Texture calculation basis

The quantitative determination of the texture is based on the concept of Orientation Distribution Function, ODF, $f(g)$, which represents the statistical distribution of the orientations of the crystallites in a polycrystalline aggregate (Chateigner et al. 2019).

The ODF is calculated from poles figures, measured by X-ray or neutron diffraction. For cubic metals three pole figures are required for calculating any ODF. Any ODF calculation needs to solve the fundamental equation of texture analysis which links the pole densities $P_h(y)$ to the texture function ODF (Suwas and Ray 2014):

$$P_h(y) = \frac{1}{2\pi} \int_{h//y} f(g) d\varphi \quad (1)$$

with: $h = \langle hkl \rangle^*$ is the crystallographic direction $[hkl]$ and diffracting equivalents of the reciprocal space, $y = (\vartheta_y, \varphi_y)$ where ϑ_y and φ_y are the spherical coordinates of the normal to diffracting plane in the specimen frame. $d\varphi$: differential element of a rotation around the normal of the diffracting plane.

Two approaches to determine the ODF from a set of pole figures, the harmonic method and vector methods were developed (Engler and Randle 2010).

2.1 Harmonic method

The solution proposed by Bunge and Esling (1982) consists in developing the ODF and the pole figures into series of generalized spherical harmonics:

$$f(g) = \sum_{\lambda=0}^{\infty} \sum_{m,n=-\lambda}^{\lambda} C_{\lambda}^{mn} T_{\lambda}^{mn}(g) \quad (2)$$

The equation (1) still holds, and in this approach, one has to determine the C_{λ}^{mn} Fourier coefficients from the experiments, which are the proportions of the respective T_{λ}^{mn} . The T_{λ}^{mn} are known generalised spherical harmonics which depend on the crystal and texture symmetries.

2.2 Vector method

The vector method (Ruer 1976; Ruer and Baro 1977; Vadon 1981; Ivankina and Matthies 2015) is a discrete method which works in the direct space. In this method $f(g)$ is represented by a vector called "Texture vector" f_j , $j: 1 \dots J$, with the J the number of cells in which $f(g)$ is discretized. In this method each pole figure is represented by $P_i(h)$, $i: 1 \dots N$, with N the number of cells of the pole figure.

The choice of discretization mode led to the development of various discrete methods which are:

- Arbitrarily Defined Cells (ADC) method (Pawlik 1993).
- Component Method (Helming 1998).
- The WIMV (Williams-Imhof-Matthies-Vinel) method (Williams 1968; Imhof 1982; Matthies and Vinel 1982; Wenk 1985; Matthies 2002) for the refinement of ODF is an iterative way which ensures a conditional ghost correction. It is based on the numerical refinement of $f(g)$ at step $n+1$:

$$f^{n+1}(g) = N_n \frac{f^n(g)f^0(g)}{\left(\prod_{h=1}^I \prod_{m=1}^{M_h} P_h^n(y)\right)^{\frac{1}{M_h}}} \quad (3)$$

Where the product extends over the I experimentally measured pole figures and for all the poles multiplicity M_h , $f^n(g)$ and $P_h^n(y)$ represent the refined values of $f(g)$ and $P_h(y)$ at the n^{th} step respectively. The number N_n is a normalizing factor. The $P_h^n(h)$ values are calculated at

each cycle with equation (1). The first step in this procedure is to evaluate $f^0(g)$ in which $P_h^{exp}(y)$ stands for the measured pole figures:

$$f^0(g) = N_0 \left(\prod_{h=1}^I \prod_{m=1}^{M_h} P_h^{exp}(y)\right)^{\frac{1}{M_h}} \quad (4)$$

The ADC method is essentially based on the WIMV algorithm, it uses projection tubes which depend on the pole figure cells of concerns.

In the component method, the texture is described by a set of discrete components. The adjustments are made on the pole figures where Gaussian function of the density distribution for each ideal orientation, is defined by: i) its center, ii) its large full-width at half-maximum (dispersion around the ideal orientation) and iii) its weight.

3 Material and texture analysis

The material used in this study was high purity copper (99.999%). The samples were cold rolled to 70% reduction in thickness and subsequently annealed under vacuum at 450 °C for various times until 100 h of annealing.

Four samples have been selected for texture analysis corresponding to the deformed state by cold rolling and subsequently annealed for 1 min, 30 min and 100 h.

Incomplete pole figures of the samples were measured by X-ray diffraction in an X’Pert PHILIPS PW 3710 diffractometer. The experimental data were corrected for background and defocusing error.

The complete pole figures, ODF and the volume fraction of texture components were calculated using Harmonic method implemented in popLA package (Kallend et al. 1991) and the ADC method (Pawlik et al. 1991).

The quantitative volume fractions of the texture components were calculated via the Harmonic method using the "Weights files" and a home made software that

enables the conversion to volume fractions of the equivalents weighted orientations. For the ADC methods, the "Integration Method" taking into account the overlapping of the texture components implemented in LaboTex Software [www.Labotex.com] has been considered.

4 Results and interpretations

The recalculated {111} poles figures using the harmonic and ADC methods of the samples in the deformed and final state (100 h of annealing) are illustrated in figure 1 and 2 respectively. Qualitatively, there is generally agreement between the iso-intensity levels in the pole figures recalculated from the harmonic and ADC methods for both samples. However, a slight decrease in the maximum intensity of pole figure obtained by the ADC method compared to that obtained by harmonic methods (Figs 1 and 2) is depicted.

It is known in the literature that the harmonic method overestimates the pole figure (Caleyo et al. 2001). In order to deeply highlight the evolution of texture of the cold rolled copper during annealing only the results obtained by the ADC method were considered. Figures 3 et 4 present the sections at $\varphi_2 = 0, 45$ and 65° of the ODF of cold rolled copper and annealed at 450°C for 100h.

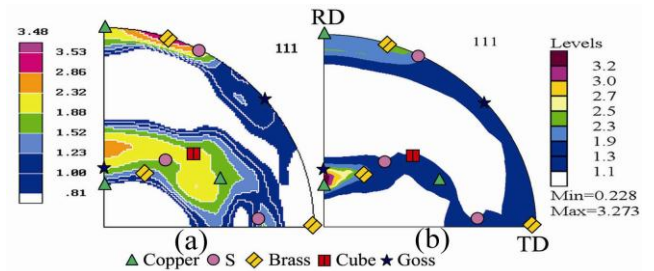


Fig. 1 Recalculated {111} poles figures of cold rolled copper obtained by: a) Harmonic method and b) ADC method.

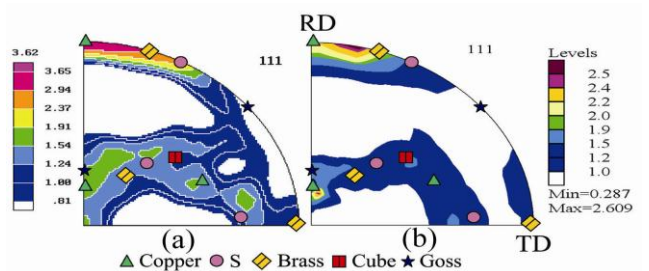


Fig. 2 Recalculated {111} poles figures of cold rolled and annealed copper at 450°C for 100h obtained by: a) Harmonic method and b) ADC method.

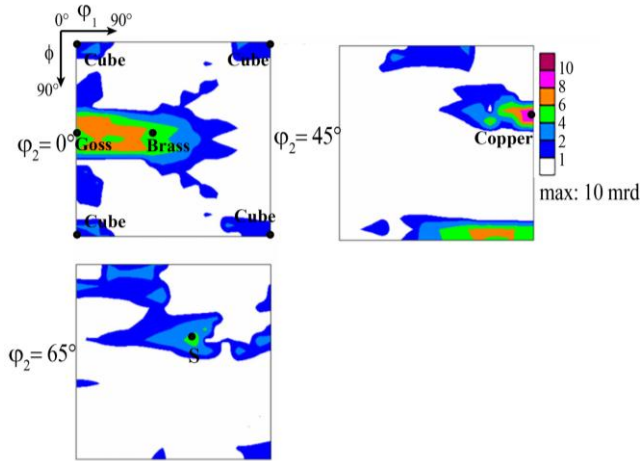


Fig. 3 Section at $\varphi_2 = 0, 45$ and 65° of the ODF of cold rolled copper obtained by ADC method.

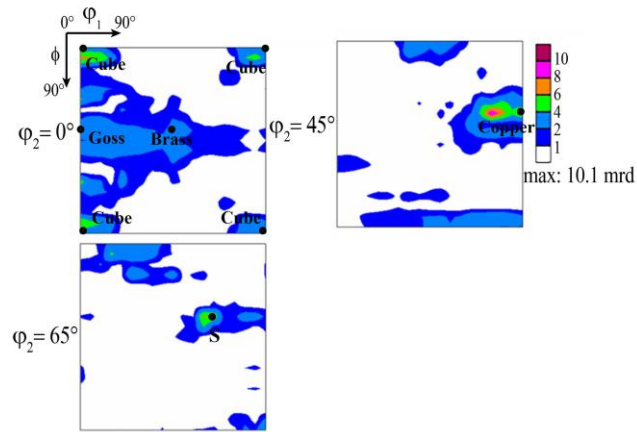


Fig. 4 Section at $\varphi_2 = 0, 45$ and 65° of the ODF of cold rolled copper and annealed at 450°C for 100 h obtained by ADC method.

The main ideal texture component positions of FCC metals are also presented and their descriptions are given in Table 1.

As pointed out by Gerber (2002), texture of cold rolled copper can be fully described by a set of five components namely Cube $\{001\}\langle 100\rangle$, Brass $\{011\}\langle 211\rangle$, S $\{123\}\langle 634\rangle$, Copper $\{112\}\langle 111\rangle$ and Goss $\{110\}\langle 001\rangle$. These components are all present in the deformed state, intermediate states (1 and 30 min of annealing) and final state (100 h annealing). The latter state exhibited a relatively sharp texture components however with the presence of stable four other texture components. Moreover, beside the Copper component at 15° away, appeared an unusual $\{112\}\langle -2-43\rangle$ component that was not considered in the further quantitative calculations. Plausibly this component may be due to shearing in the rolling direction (RD).

Table 1 Main ideal rolling texture components of FCC metals.

Component	$\{hkl\}\langle uvw\rangle$	Euler Angle		
		φ_1	Φ	φ_2
Brass	$\{110\}\langle 112\rangle$	35°	35°	45°
Goss	$\{110\}\langle 001\rangle$	0°	45°	0°
Cube	$\{001\}\langle 100\rangle$	0°	0°	0°
Copper	$\{112\}\langle 111\rangle$	90°	35°	45°
S	$\{231\}\langle 346\rangle$	59°	29°	63°

Quantitative results of the texture of the studied samples by the harmonic and ADC methods, are shown in Table 2. It is noted that Harmonic method resulted in erroneous values of volume fraction of the Copper and the S texture components. The values of volume fraction of Cube, Brass and Goss components obtained by the ADC and harmonic methods for the deformed state, intermediate states (1 and 30 min of annealing) and final state (100 h annealing) are very close. Indeed, we note that the volume fraction values of the deformed state are not in good agreement with those presented by Gerber (2002) in 70% cold rolled copper oxygen free electronic (OFE). Moreover, in our opinion, the results of Gerber overestimated the volume fraction, the decreasing order of volume fraction of all texture components was not well respected ($S > \text{Brass} > \text{Cube} > \text{Goss} > \text{Copper}$ while for Gerber's study $\text{Cube} > \text{Copper} > \text{Brass} > S > \text{Goss}$).

After one 1 min of annealing, the volume fraction of all texture components remained almost constant compared to those of the deformed state. After 30 min of annealing the volume fraction of the Brass and S components significantly decreased, when the Cube component decreases slightly keeping always the higher weight. This led to recrystallization texture dispersed relatively (maximum intensity of pole figure = 1.37). This type of texture was similar to that observed by Gerber (2002) and Necker (1997) after recrystallization of copper deformed after cold rolling with strain level close to that imposed in this study.

The absence of sharp Cube texture in the fully recrystallized state can ascribed to the twinning process which strongly contributes to widespread the texture through the emergence of new orientations during annealing (Gottstein 1984; Necker 1997; Baudin 2003) and also to strain level imposed to the material.

Table 2 Volume fraction of texture components of the studied samples calculated by Harmonic and ADC methods.

Texture component	Cold rolled (CR)		CR + annealed for 1 min		CR + annealed for 30 min		CR + annealed for 100 h	
	Harmonic method	ADC method	Harmonic method	ADC method	Harmonic method	ADC method	Harmonic method	ADC method
Cube	7.7	10.6	9.9	14.8	12.3	11.2	10.6	13.4
Brass	6.6	14.2	9.5	11.8	6.8	5.5	9.5	8.9
Goss	5.8	9.8	6.3	7.3	6.4	5.8	5.9	6.4
Copper	-	7.7	-	10.0	-	7.2	-	10.4
S	-	16.2	-	10.6	-	6.6	-	10.0

About the influence of the last factor, it has been demonstrated that the cold rolled copper sample presents a deformation threshold below which the recrystallization texture is relatively dispersed, while for a value equal or greater the recrystallization texture is dominated by the orientation Cube (Necker et al. 1995; Gerber 2002).

However, the texture after the process of grain growth (after 100 h of annealing) did not present much difference compared to that of fully recrystallized state (after 30 min annealing). In the final state, the texture components slightly increased and caused the appearance of an isotropic texture less dispersed (maximum intensity of pole figure = 2.60).

Moreover, in a previous work of the same material (Benchabane et al. 2011), the microstructure of the fully recrystallized and the final state were characterized by Electron Back Scatter Diffraction (EBSD). The results showed that the fully recrystallized state presented an important fraction of twins which was attributed to the twinning process. Additional annealing at 450 °C for 100 h caused the grain growth and a decrease of the twin fraction.

5 Conclusion

The texture analysis of a cold rolled and annealed pure copper using the harmonic and the ADC methods, have been presented.

In qualitative texture analysis, it has been shown that the two methods reproduced similar recalculated pole figures. In addition, quantitative texture analysis have shown that the ODF and volume fraction of texture components obtained by the ADC and harmonic methods are very close.

The texture evolution of the cold rolled copper during annealing can be summarized in the following points:

- The sharpness of the deformation texture decreased during annealing leading to a dispersed texture in fully recrystallized state (30 min of annealing).
- The texture after the process of grain growth (100 h annealing) was isotropic and less dispersed compared to the fully recrystallized state.

Acknowledgment

Authors are thankful to Professors T. Gloriant and I. Thibon (University of Rennes, INSA Rennes, CNRS, SCR—UMR 6226) for their help and assistance. One of the authors (D.B.) heartily acknowledges U.F. Kocks from the Los Alamos National Laboratory for making the PopLA package available.

References

- Bacroix, B., Th. Chauveau, P. Gargano, A.A. Pochettino (1994) Some comments about texture analysis: comparison between harmonic and vector methods. *Materials Science Forum* 157-162: 301-308.
- Baudin, T., A. Vadon, R. Penelle, J.J. Heizmann (1995) Caractérisation de la texture de recristallisation primaire d'une tole de Fe3%Si (nuance HiB). *Journal de Physique IV 05 (C3): C3-285-C3-290.*
- Baudin, T., F. Julliard, R. Penelle (2003) Recrystallization texture development by multiple twinning in the Invar (Fe-36 %Ni) alloy. *Revue de Métallurgie* 100(2): 193-202.
- Benchabane, G., Z. Boumerzoug, I. Thibon, T. Gloriant (2008) Recrystallization of pure copper investigated by calorimetry and microhardness. *Materials Characterization* 59(10): 1425-1428.

- Benchabane, G., Z. Boumerzoug, T. Gloriant, I. Thibon (2011) Microstructural characterization and recrystallization kinetics of cold rolled copper. *Physica B: Condensed Matter* 406(10): 1973-1976.
- Bunge, H.J. (1965) Zur darstellung allgemeiner texturen. *Z. Metallkunde* 56: 872-874.
- Bunge, H.J. (1982) *Texture Analysis in Materials Science. Mathematical Methods.* London, Butterworths and CO (Publishers).
- Bunge, H.J., C. Esling (1982) *Quantitative Texture Analysis.* Ed. H.J. Bunge and C. Esling, Germany, DGM.
- Caleyo, F., T. Baudin, M.H. Mathon, R. Penelle (2001) Comparison of several methods for the reproduction of the orientation distribution function from pole figures in medium to strong textured materials. *The European Physical Journal Applied Physics* 15(2): 85-96.
- Chateigner, D., L. Lutterotti, M. Morales (2019) Quantitative texture analysis and combined analysis, in *International Tables for Crystallography. Vol. H, Chapter 5.3.* Ed. C. J. Gilmore, J. A. Kaduk and H. Schenk, International Union of Crystallography, pp. 555-580.
- Engler, O., V. Randle (2010) *Introduction to texture analysis: macrotexture, microtexture, and orientation mapping: Second Edition.* Boca Raton, CRC press.
- Esling, C., H.J. Bunge, M.J. Philippe, J. Muller (1987) *Theoretical Methods of Texture Analysis.* Ed. H.J. Bunge, Oberursel, DGM.
- Gerber, Ph. (2002) *Etude des liens entre hétérogénéités de déformation et mécanismes de recristallisation. Application au cuivre et ses alliages.* PhD Thesis, Université de Paris XIII, Villetaneuse, France.
- Gottstein, G. (1984) Annealing texture development by multiple twinning in fcc crystals. *Acta Metallurgica* 32(7): 1117-1138.
- Helming, K. (1998) Texture approximations by model components. *Materials Structure* 5(1): 3-9.
- Imhof, J. (1982) The resolution of orientation space with reference to pole figure resolution. *Textures and Microstructures* 4: 189-200.
- Ivankina, T.I., S. Matthies (2015) On the development of the quantitative texture analysis and its application in solving problems of the earth sciences. *Physics of Particles and Nuclei* 46(3): 366-423.
- Kallend, J.S., U.F. Kocks, A.D. Rollett, H.R. Wenk (1991) *Operational texture analysis.* *Materials Science and Engineering: A* 132: 1-11.
- Kocks, U.F., C.N. Tomé, H.R. Wenk (2000) *Texture and Anisotropy. Preferred Orientations in Polycrystals and Their Effect on Materials Properties.* 2nd paperback Ed. Cambridge University Press, Cambridge.
- Matthies, S., G.W. Vinel (1982) On the reproduction of the orientation distribution function of textured samples from reduced pole figures using the concept of conditional ghost correction. *Physica Status Solidi B* 112: K111-114.
- Matthies, S., H.R. Wenk, G.W. Vinel (1988) Some basic concepts of texture analysis and comparison of three methods to calculate orientation distributions from pole figures. *Journal of Applied Crystallography* 21(4): 285-304.
- Matthies, S., (2002) 20 years WIMV, history, experience and contemporary developments. *Materials Science Forum* 408-412: 95-100.
- Necker, C.T., R.D. Doherty, A.D. Rollet (1995) The development of cube and non-cube recrystallization textures. *Proceedings of the 16th Risø International Symposium on Materials Science*, Eds. N. Hansen et al., Roskilde, Denmark.
- Necker, C.T. (1997) *Recrystallization texture in cold rolled copper.* PhD Thesis, Drexel University, United States of America.
- Pawlik, K., J. Pospiech, K. Lücke (1991) The ODF approximation from pole figures with the aid of the ADC method. *Textures and Microstructures* 14-18: 25-30.
- Pawlik, K. (1993) Application of the ADC method for ODF approximation in cases of low crystal and sample symmetries. *Materials Science Forum* 133-136: 151-156.
- Rafailov, G., E.A.N. Caspi, R. Hielscher, E. Tiferet, R. Schneck, S.C. Vogel (2020) Visualization of texture components using MTEX. *Journal of applied crystallography* 53(2): 540-548.

- Roe, R.J. (1965) Description of crystalline orientation of polycrystalline materials. III. General solution to pole figure inversion. *Journal of Applied Physics* 36(6): 2024–2031.
- Roe, R.J. (1966) Inversion of pole figures for materials having cubic crystal symmetry. *Journal of Applied Physics* 37(5): 2069-2072.
- Ruer, D. (1976) Méthode vectorielle d'analyse de la texture. PhD Thesis, Université Paul Verlaine-Metz, France.
- Ruer, D., R. Baro (1977) A new method for the determination of the texture of materials of cubic structure from incomplete reflection pole figures. *Advances in X-ray Analysis* 20: 187-200.
- Suwas, S., R.K. Ray (2014) Representation of Texture, in *Crystallographic Texture of Materials*. Engineering Materials and Processes, London, Springer, pp. 11-38.
- Vadon, A. (1981) Généralisation et optimisation de la méthode vectorielle d'analyse de la texture. PhD Thesis, Université de Metz, France.
- Wenk, H.R. (1985) Preferred Orientation in Deformed Metals and Rocks: An Introduction to Modern Texture Analysis. Ed. H.R. Wenk, San Diego, Academic Press.
- Wenk, H.R., H.J. Bunge, J.S. Kallend, K. Lücke, S. Matthies, J. Pospiech, P. Van Houtte (1987) Orientation distributions. Representation and determination. Proceedings of ICOTOM8. Ed. J. Kallend and G. Gottstein, The Metallurgical Society, Warrendale, Pennsylvania, pp. 17-30.
- Wenk, H.R., P. Van Houtte (2004) Texture and anisotropy. *Reports on Progress in Physics* 67(8): 1367-1428.
- Williams, R.O. (1968) Analytical methods for representing complex textures by biaxial pole figures. *Journal of Applied Physics* 39(9): 4329-4335.